ELSEVIER

The American Journal of
PATHOLOGY

ajp.amjpathol.org

IMMUNOPATHOLOGY AND INFECTIOUS DISEASES

Natural Killer Cells Limit Cardiac Inflammation and Fibrosis by Halting Eosinophil Infiltration

SuFey Ong,* Davinna L. Ligons,† Jobert G. Barin,† Lei Wu,* Monica V. Talor,† Nicola Diny,* Jillian A. Fontes,* Elizabeth Gebremariam,† David A. Kass,‡ Noel R. Rose,*† and Daniela Čiháková*†

From The W. Harry Feinstone Department of Molecular Microbiology and Immunology,* Johns Hopkins University, Bloomberg School of Public Health, Baltimore; and the Departments of Pathology† and Cardiology,‡ Johns Hopkins University School of Medicine, Baltimore, Maryland

Myocarditis is a leading cause of sudden cardiac failure in young adults. Natural killer (NK) cells, a subset of the innate lymphoid cell compartment, are protective in viral myocarditis. Herein, we demonstrated that these protective qualities extend to suppressing autoimmune inflammation. Experimental autoimmune myocarditis (EAM) was initiated in BALB/c mice by immunization with myocarditogenic peptide. During EAM, activated cardiac NK cells secreted interferon γ, perforin, and granzyme B, and expressed CD69, tumor necrosis factor—related apoptosis-inducing ligand treatment, and CD27 on their cell surfaces. The depletion of NK cells during EAM with anti-asialo GM1 antibody significantly increased myocarditis severity, and was accompanied by elevated fibrosis and a 10-fold increase in the percentage of cardiac-infiltrating eosinophils. The resultant influx of eosinophils to the heart was directly responsible for the increased disease severity in the absence of NK cells, because treatment with polyclonal antibody asialoganglioside GM-1 did not augment myocarditis severity in eosinophil-deficient ΔdoubleGATA1 mice. We demonstrate that NK cells limit eosinophilic infiltration both indirectly, through altering eosinophil-related chemokine production by cardiac fibroblasts, and directly, by inducing eosinophil apoptosis *in vitro*. Altogether, we define a new pathway of eosinophilic regulation through interactions with NK cells. *(Am J Pathol 2015, 185: 847—861; http://dx.doi.org/10.1016/j.ajpath.2014.11.023)*

Myocarditis is a leading cause of sudden cardiac failure in individuals <40 years, with 9% to 16% of cases progressing to inflammatory dilated cardiomyopathy.[1–3] Necrotizing eosinophilic myocarditis, a subset of myocarditis, is characterized by extensive cardiac eosinophilic infiltration, pronounced cardiomyocyte death, and higher fatality rates.[4–9] Correlations between eosinophil frequency and poor clinical outcomes have been reported in other chronic inflammatory disease models, including asthma, inflammatory bowel disease, and experimental autoimmune encephalomyelitis.[10–12] Herein, we investigated the connection between eosinophils and natural killer (NK) cells, highlighting a new pathway responsible for the control of eosinophilic accumulation in sites of inflammation.

Our group and others have reported that NK cells, an innate lymphoid cell subset, are protective in coxsackievirus B3 and murine cytomegalovirus animal models of myocarditis by limiting viral replication.[13–15] Because myocarditis is also an autoimmune-mediated disease, it is unknown if NK cells can protect against disease through limiting viral replication, as well as by reducing the autoimmune response.[16,17] The data regarding NK cells and autoimmunity are extensive, but conflicting. NK cells accumulate in joints during rheumatoid arthritis (RA), skin lesions during psoriasis, and brain lesions during multiple sclerosis.[18,19] Activated NK cells from the joints of RA patients induce differentiation of monocytes, signifying an active role in the immune environment,[20] and indicating that NK cells play a proinflammatory role in autoimmunity.

This directly contradicts the observations that myocarditis, RA, Sjögren syndrome, and systemic lupus erythematosus patients have decreased NK cell numbers and cytotoxicity potential.[21−25] A limited study of biopsy specimens from myocarditis patients revealed a lack of NK cells in the cardiac tissue.[26] Peripheral NK cells from RA patients failed to induce apoptosis in major histocompatibility complex I−deficient K562 cells versus healthy controls *in vitro*. Patients with multiple sclerosis in remission had higher frequencies of activated peripheral NK cells than those with active disease, supporting the notion that defects in NK cells are associated with increased risk of autoimmunity.[27] Altogether, it is unclear whether autoimmune diseases are exacerbated by deficiencies or excesses of NK cells, making animal studies necessary.

Herein, we investigated the role of NK cells in autoimmune myocarditis using a mouse model of experimental autoimmune myocarditis (EAM). EAM is induced by s.c. immunization of myocarditogenic peptide in complete Freund's adjuvant, the same antigen targeted by autoaggressive T cells in coxsackievirus group B type 3 (CB3)-induced myocarditis.[28−31] Susceptible mice strains develop myocarditis, followed by inflammatory dilated cardiomyopathy.[29] EAM induces the immune response independent of persistent virus, allowing us to separate autoimmune- from virus-mediated disease. We report herein the ability of NK cells to control myocarditis in the absence of a viral pathogen.

Materials and Methods

Mice

BALB/c, $Rag1^{-/-}$, C.Cg-$Gata1^{tm6Sho}$/J (ΔdoubleGATA1), CD3δ-IL5Tg NJ.1636, $Ccr3^{-/-}$, interferon γ receptor 1 (IFNγR1)$^{-/-}$, and IFNγ$^{-/-}$ mice were purchased from the Jackson Laboratory (Bar Harbor, ME) and were bred and maintained in the conventional housing facilities at Johns Hopkins University (Baltimore, MD). All protocols have been reviewed and approved by the Johns Hopkins Animal Care and Use Committee.

Immunization with MHC$_{614-629}$ and Assessment of EAM

Male 6- to 8-week-old BALB/c mice were injected s.c. with 100 μg of myocarditogenic peptide of cardiac myosin heavy chain (MyHC), MyHC$_{614-629}$, emulsified in an equal volume of complete Freund's adjuvant (Sigma-Aldrich, St. Louis, MO), supplemented with 4 mg/mL of H37Ra extract (Difco, Lawrence, KS) on days 0 and 7, as previously described.[29] Pertussis toxin (500 ng in 100 μL of phosphate-buffered saline (PBS; Sigma-Aldrich) was administered i.p. on day 0. Mice were sacrificed on day 21; hearts were collected and sections were stained with hematoxylin and eosin, as previously described.[32−35] The degree of myocardial infiltration and fibrosis was determined blindly by two individuals (D.C.

and S.O.), and histology was scored as follows: 0, no infiltration; 1, ≤10%; 2, 11% to 30%; 3, 31% to 50%; 4, 51% to 90%; and 5, >90%.[29]

Assessment of Fibrosis

Mice were sacrificed on day 21. Hearts were collected and sections were stained with Masson's trichrome, as previously described.[32−35] Images of Masson's trichrome−stained cardiac sections were uploaded into ImageJ software version 1.48 (NIH, Bethesda, MD). The background space was deleted and the left ventricle, the region of interest, was selected using the freeform loop tool. Pixels within the selected area were deconstructed into red (tissue) or blue (collagen) channels, and fibrosis was calculated as a percentage of blue versus total red plus blue pixels in the region of interest.

Echocardiography

An Acuson Sequoia 256 high-resolution microimaging system with a 13-MHz transducer was used (Visualsonic, Toronto, ON, Canada). In conscious mice, the heart was imaged in the two-dimensional mode in the parasternal short-axis view. From the M-mode, the left ventricular (LV) wall thickness and chamber dimensions were measured. The M-mode cursor was positioned perpendicular to the intraventricular septum and the LV posterior wall, with three to five readings taken for each measurement. The LV end diastolic dimension, LV end systolic dimension, LV posterior wall thickness at end diastole, and the intraventricular septal wall thickness at end diastole were measured from a frozen M-mode tracing. Fractional shortening, ejection fraction, and relative wall thickness were calculated as previously described.[32]

Intracardiac and Splenic Flow Cytometry

The aorta was cannulated to perfuse hearts with 15 mL of cold 1× PBS for 3 minutes to remove blood. To generate cardiac single-cell suspensions, hearts were bisected, placed in C-tubes, and dissociated on the GentleMACS system (Miltenyi Biotech, Bergisch Gladbach, Germany) under program heart_01. Cells were placed in a rotating incubator with 10 mg of collagenase II and 1.5 mg of DNase I (Worthington Biochemical, Lakewood, NJ) for 30 minutes at 37°C. Cells were dissociated again and rinsed twice with 1× PBS with 0.05% bovine serum albumin (BSA; Sigma-Aldrich) and 2 mmol/L EDTA (Corning Cellgro, Corning, NY). To generate a splenic single-cell suspension, spleens were dissociated between two frosted glass slides and incubated with 2 mL of ACK Lysing Buffer for 1 minute. The cells were rinsed with 1× PBS (Mediatech, Manassas, VA) and filtered through a 40-μm mesh. Cells (1 to 3 × 10^6) were incubated with 1 μL of LIVE/DEAD Aqua (Invitrogen, Carlsbad, CA) for 30 minutes in 1× PBS to stain

dead cells. Cells were then incubated with 2 µg of αCD16/32 at 4°C for 10 minutes before the addition of fluorescent antibodies (CD3, CD4, CD8, CD45, Ly6G, SiglecF, NKp46, DX5, CD11b, CD11c, and F4/80) (eBioscience, San Diego, CA). Samples were incubated with antibodies at 4°C for 10 to 20 minutes, washed in 1 mL of 0.5% BSA in 1× PBS, and fixed in fixation and permeabilization buffer (BD Bioscience, Franklin Lakes, NJ) for 30 minutes. For intracellular cytokine staining, suspensions were incubated for 4 to 6 hours with 20 ng/mL 4β-phorbol 12-myristate 13-acetate, 1 µg/mL ionomycin, and Golgistop (BD Bioscience). Cells were surface stained and then permeabilized with 1× permeabilization buffer (BD Bioscience) overnight at 4°C. Cells were then incubated with anti-cytokine antibodies (eBioscience) for 30 minutes at 4°C. Cells were washed in 1× permeabilization buffer and resuspended in 100 to 200 µL of buffer. Samples were acquired on the LSR II quad-laser cytometer running FACSDiva 6 (BD Immunocytometry, Franklin Lakes, NJ). Data were analyzed with FlowJo version 7.6 (Treestar Software, Ashland, OR).

Depletion of NK Cells with Anti-Asialo GM1 Antibody

To deplete NK cells before immunization, 6-week-old male BALB/c mice were injected i.p. with 1 mg of anti-asialo GM1 (Wako Chemicals USA, Richmond, VA) antibody every day 6 days before the first immunization (days -6 to 0).[36,37] To maintain decreased levels of NK cells after the first immunization (day 0), 1 mg of anti-asialo GM1 antibody was administered every other day until day 20. Control mice received 1 mg of rabbit IgG (Sigma-Aldrich) by the same schedule.

Isolation of Primary Adult Mouse Cardiac Fibroblasts

Primary adult mouse cardiac fibroblasts were isolated with minor modifications from protocols previously described.[38] Hearts dissected from 6- to 8-week-old naïve BALB/c mice were perfused through the aorta with warmed 37°C calcium-free buffer, followed by collagenase type II (Worthington Biochemical, Lakewood, NJ) for 15 minutes. Tissue was dissolved into a single-cell suspension and filtered through a 70-µm mesh. Cells were seeded, and nonadherent cells were washed off after 1 hour. Cells were either collected immediately in TRIzol reagent (Invitrogen) for *ex vivo* experiments or passaged twice before *in vitro* use in complete Dulbecco's modified Eagle's medium with 20% fetal bovine serum (Hyclone Laboratories, Logan, UT), 1× penicillin/streptomycin, 25 mmol/L HEPES, 1× Anti-Anti (Gibco, Carlsbad, CA), and 1× nonessential amino acids.

Isolation of Primary NK Cells

NK cells were negatively isolated from $Rag1^{-/-}$ BALB/c spleens by manual magnetic cell sorting using the Mouse NK Isolation Kit II (Miltenyi Biotech) and cultured for 24 hours with 10 ng/mL IL-12 and 5 ng/mL IL-15.

Isolation of Primary Eosinophils

Eosinophils were isolated from naïve CD3δ-IL5Tg NJ.1636 peripheral blood mononuclear cells using a Percoll (GE Lifesciences, Marlborough, MA) gradient and subsequent negative fluorescence-activated cell sorting for $SSC^{hi}Ly6G^-DX5^-$ eosinophils.

Apoptosis Measurement

Cells were harvested from culture and rinsed twice with 1× PBS with 0.05% BSA (Sigma-Aldrich) and 2 mmol/L EDTA (Corning Cellgro). The cells were rinsed with 1× PBS and incubated with 1 µL of LIVE/DEAD Aqua (Invitrogen) for 30 minutes in 1× PBS to stain dead cells. Cells were then incubated with 2 µg of αCD16/32 at 4°C for 10 minutes before the addition of fluorescent antibodies (Ly6G, SiglecF, and NKp46) (eBioscience). Samples were incubated with antibodies at 4°C for 10 to 20 minutes and washed in 1 mL of 0.5% BSA in 1× PBS. Cells were then resuspended in 1× Annexin Binding Buffer (eBioscience) and stained with 2 µL of annexin V. Cells were acquired after 15 minutes of incubation on ice on the LSRII flow cytometer (Becton Dickenson, Franklin Lakes, NJ).

mRNA

For real-time quantitative PCR (qPCR), cells or tissues were homogenized in TRIzol reagent and chloroform extracted. Samples were DNase treated, and cDNA libraries were made using iScript Reverse Transcriptase Supermix (Bio-Rad, Hercules, CA). mRNA was amplified using SYBR Green (Applied Biosystems, Foster City, CA), and all values were calculated against hypoxanthine-guanine phosphoribosyltransferase (HPRT) mRNA. Values were controlled against isotype control groups and shown as a function of fold induction using the formula $2^{-\Delta(\Delta C_T)}$.

Murine primers were as follows (forward and reverse primers, respectively): Hprt, 5′-TCCTCCTCAGACCGCT-TTT-3′ and 5′-TCTGCTGGAGTCCCCTTG-3′; collagen 1a1 (Col1a1), 5′-AGCAGGTCCTTGGAAACCTT-3′ and 5′-AAGGAGTTTCATCTGGCCCT-3′; Col1a2, 5′-GTGAAC-GGGGCGAAGCTGGTT-3′ and 5′-GCGGCTCCTGGAA-GCCCATTTG-3′; Col1a3, 5′-AACCTGGTTTCTTCTCA-CCCTTC-3′ and 5′-ACTCATAGGACTGACCAAGGTGG-3′; Il4, 5′-AAGGCAACTTTCTTGATATT-3′ and 5′-GG-CCTTTCAGACTAATCTT-3′; Il13, 5′-TGAGGAGCT-GAGCAACATCACACA-3′ and 5′-TGCGGTTACAGAG-GCCATGCAATA-3′; eosinophil peroxidase, 5′-AGATG-CAACAACAAGAAGCATCC-3′ and 5′-TGATTGGAGA-CATCCCGGAC-3′; major basic protein 2, 5′-TGAAA-CTTCTGACTCCAAAAGCC-3′ and 5′-CGGCATTAGCT-CTTCCCCT-3′; Il1b, 5′-CAACCAACAAGTGATATTC-TCCATG-3′ and 5′-GATCCACACTCTCCAGC-TGCA-3′; transforming growth factor (Tgf) b1, 5′-CTCCCGTGGC-TTCTAGTGC-3′ and 5′-GCCTTAGTTTGGACAGGATC-TG-3′; chemokine ligand 11 (Ccl11), 5′-GAATCACCAACA-

ACAGATGCAC-3′ and 5′-TCCTGGACCCACTTCTTCTT-3′; Ccl24, 5′-TCTTAGGGCCCTTCTTGGTG-3′ and 5′-AA-TTCCAGAAAACCGAGTGG-3′; and Cxcl9, 5′-GTGGAG-ACCACCAGAGTTGG-3′ and 5′-TGCCACTAAGCTACA-GCCAC-3′.

Enzyme-Linked Immunosorbent Assays

Samples were run using tissue homogenates in $1\times$ PBS or cell culture supernatant using enzyme-linked immunosorbent assay kits for Ccl11 (RND Biosystems, Minneapolis, MN) or a multiplex LINCO kit (Millipore, Jaffery, NH).

Statistical Analysis

Multiple group comparisons were performed by ordinary one-way analysis of variance, followed by the Tukey-Kramer post test (if parametric) or Kruskal-Wallis, followed by Dunn's post test (if nonparametric) (GraphPad Prism 5; GraphPad, San Diego, CA). All statistics of two groups were performed by Student's t-test. $P < 0.05$ was considered statistically significant.

Results

NK Cells Suppress Cardiac Inflammation and Severe Myocarditis in EAM

To determine whether NK cells modulate EAM, we depleted NK cells *in vivo* using 1 mg of anti-asialoganglioside GM-1 (ASGM-1) polyclonal antibody injected i.p. from day -6 to day 21, as described in *Materials and Methods* (Figure 1A). The depletion caused myocarditis to increase in severity as assessed by histology and total count of infiltrating $CD45^+$ cells in the heart at the peak of inflammation on day 21 (Figure 1, B–D). This was accompanied by increased circulating anti−MyHCα$_{614-629}$-specific IgG antibodies (Figure 1E). At this time, ASGM-1 antibody reduced $CD3^-DX5^+NKp46^+$ NK cells, but not $CD3^+DX5^+$ NK T cells (Figure 1, F and G) in the spleen and heart during EAM. ASGM-1 had little effect on other cell types in naïve animals, because antibody treatment depleted $CD3^-DX5^+NKp46^+$ NK, but not $CD3^+DX5^+NKp46^+$, NK T cells or $Ly6G^{lo}SiglecF^+$ eosinophils (Supplemental Figure S1). Development of severe myocarditis after depletion of NK cells suggests that NK cells protect from severe cardiac inflammation.

Absence of NK Cells Increases Collagen Deposition in the Heart

We explored whether NK cells inhibit fibrosis development and inflammation. To assess fibrosis quantitatively, images of cardiac histology slides stained by Masson's trichrome were processed by ImageJ software to enumerate collagen-positive (blue) versus nonfibrotic (red) pixels. NK-depleted

animals had increased cardiac collagen deposition on day 21 of EAM (Figure 2, A and B). This accompanied a decline in cardiac function, as shown by decreased ejection fraction with increased LV end systolic diameter and no changes in LV end diastolic diameter or intraventricular septal thickness (Figure 2, C−F). We quantified active collagen production in NK-depleted mice at day 21 and showed that NK depletion led to increased mRNA levels of collagen 1 and collagen 3 in the heart (Figure 2, G−I). Thus, the depletion of NK cells during EAM leads to increased cardiac fibrosis and a decline in cardiac function.

Activated NK Cells Accumulate in the Heart during EAM

To examine NK cell kinetics during EAM, we quantified cardiac NK cells by flow cytometry (Figure 3A). $CD3^-DX5^+NKp46^+$ NK cells increased from day 0 to day 21 in absolute counts; however, their proportion out of $CD45^+$ cells was stable (Figure 3, B and C). To determine their phenotype, we profiled cytokine and receptor expression from NK cells by flow cytometry on day 21 of EAM to see if they represented an activated population compared to those in the periphery. Cardiac NK cells produced more Ifnγ than splenic NK cells, but equivalent levels of Il-13 (Figure 3, D and E). Greater proportions of cardiac NK cells up-regulated perforin and were positive for lysosomal-associated membrane protein 1 (LAMP-1), a correlate for granzyme B secretion (Figure 3, F and G). In addition, cardiac NK cells up-regulated activation markers CD27, CD69, and tumor necrosis factor−related apoptosis-inducing ligand treatment (Figure 3, H−J), with decreased NKG2D (Figure 3K). Thus, cardiac NK cells secrete Ifnγ and have increased expression of multiple activation receptors compared to NK cells in periphery during the course of myocarditis.

Activated Fibroblasts Are Not Targeted for Cytotoxic Killing by NK Cells *in Vitro*

The depletion of NK cells led to accelerated fibrosis (Figure 2) in the heart; therefore, we hypothesized that NK cells lysed activated fibroblasts, as described in animal models of liver fibrosis.[39,40] We explored this putative mechanism using a co-culture system *in vitro* with an outcome focused on cell death. First, adult cardiac fibroblasts were isolated from naïve BALB/c hearts and passaged twice. The presence of contaminating macrophages was ruled out by qPCR and immunofluorescence (Supplemental Figure S2). Second, NK cells were isolated from naïve or poly(I:C)-treated BALB/c spleens (Supplemental Figure S3A). Cardiac fibroblasts were activated with angiotensin II, illustrated by increased expression of vimentin (Supplemental Figure S3B). Finally, we co-cultured cardiac fibroblasts and NK cells together for 48 hours at a 1:1 ratio. Cardiac fibroblasts were stained green with calcein AM (live cells) and red with ethidium homo-dimer (dead cells) and examined by immunofluorescence
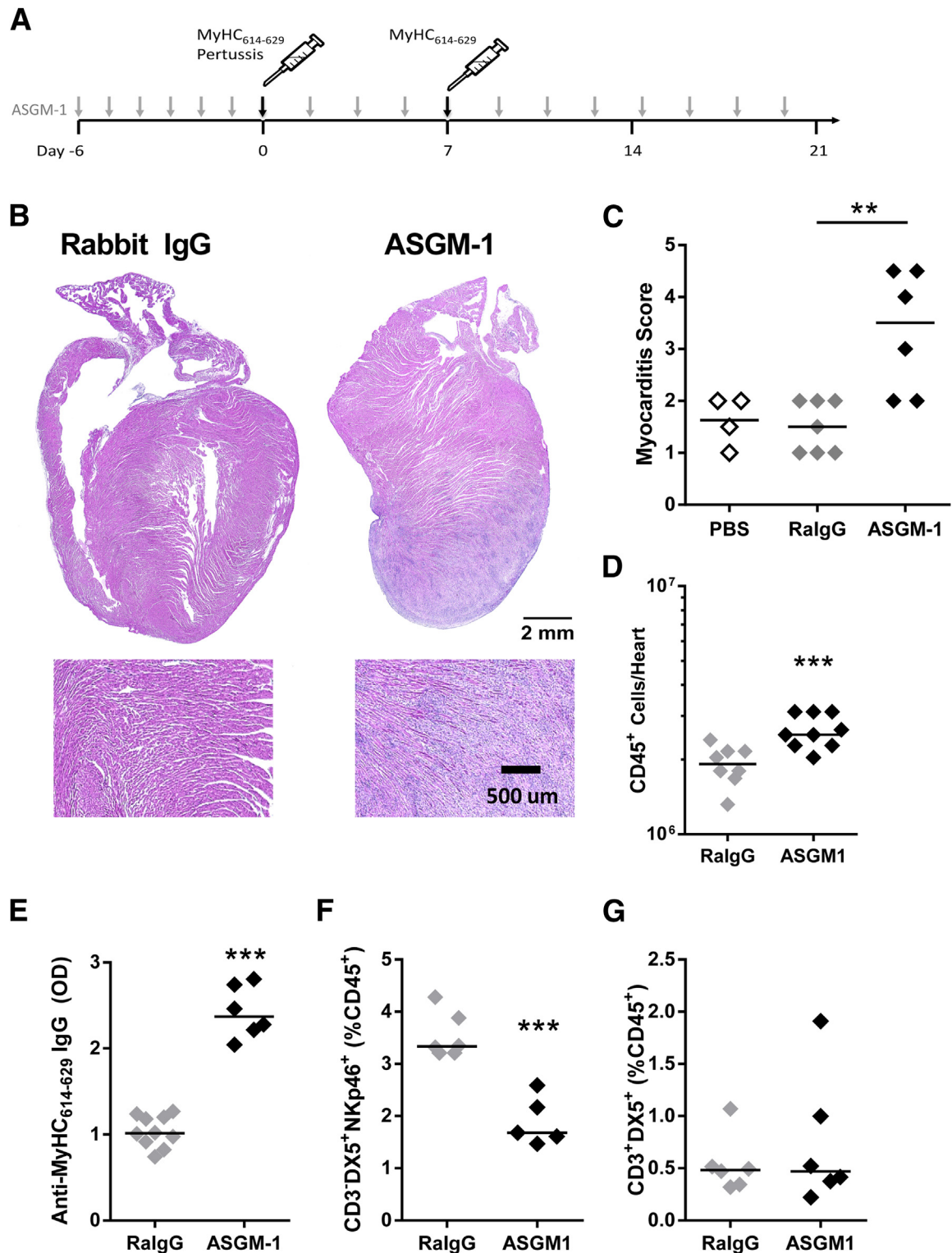
Figure 1 Depletion of natural killer (NK) cells increases cardiac inflammation and the severity of experimental autoimmune myocarditis (EAM). **A:** Schematic of phosphate-buffered saline (PBS), rabbit IgG, and asialogangloside GM-1 (ASGM-1) antibody treatment schedule throughout EAM. Representative histology from rabbit IgG (RaIgG) and ASGM-1—treated animals (**B**) and scores of hematoxylin and eosin—stained cardiac sections from PBS, rabbit IgG, and ASGM-1 antibody treated animals at day 21 of EAM (analysis of variance $P < 0.01$; **C**). **D:** Total CD45$^+$ cells infiltrating the hearts of isotype control and ASGM-1—treated animals at day 21 of EAM, as assessed by flow cytometry ($P < 0.001$). **E:** Levels of anti-myocarditogenic peptide of cardiac myosin heavy chain (MyHC)$_{614-629}$ total IgG antibodies in the serum of PBS, isotype control, and ASGM-1—treated animals at day 21 of EAM (analysis of variance $P < 0.001$). Percentage of CD3$^-$DX5$^+$NKp46$^+$ NK cells in the heart ($P < 0.001$) and spleen ($P < 0.002$) (**F**) and CD3$^+$DX5$^+$ NK T cells out of CD45$^+$ cells (**G**) of rabbit IgG and ASGM-1 monoclonal antibody—treated wild-type (WT) mice at day 21 of EAM, as assessed by flow cytometry. **P < 0.05, ***P < 0.001.
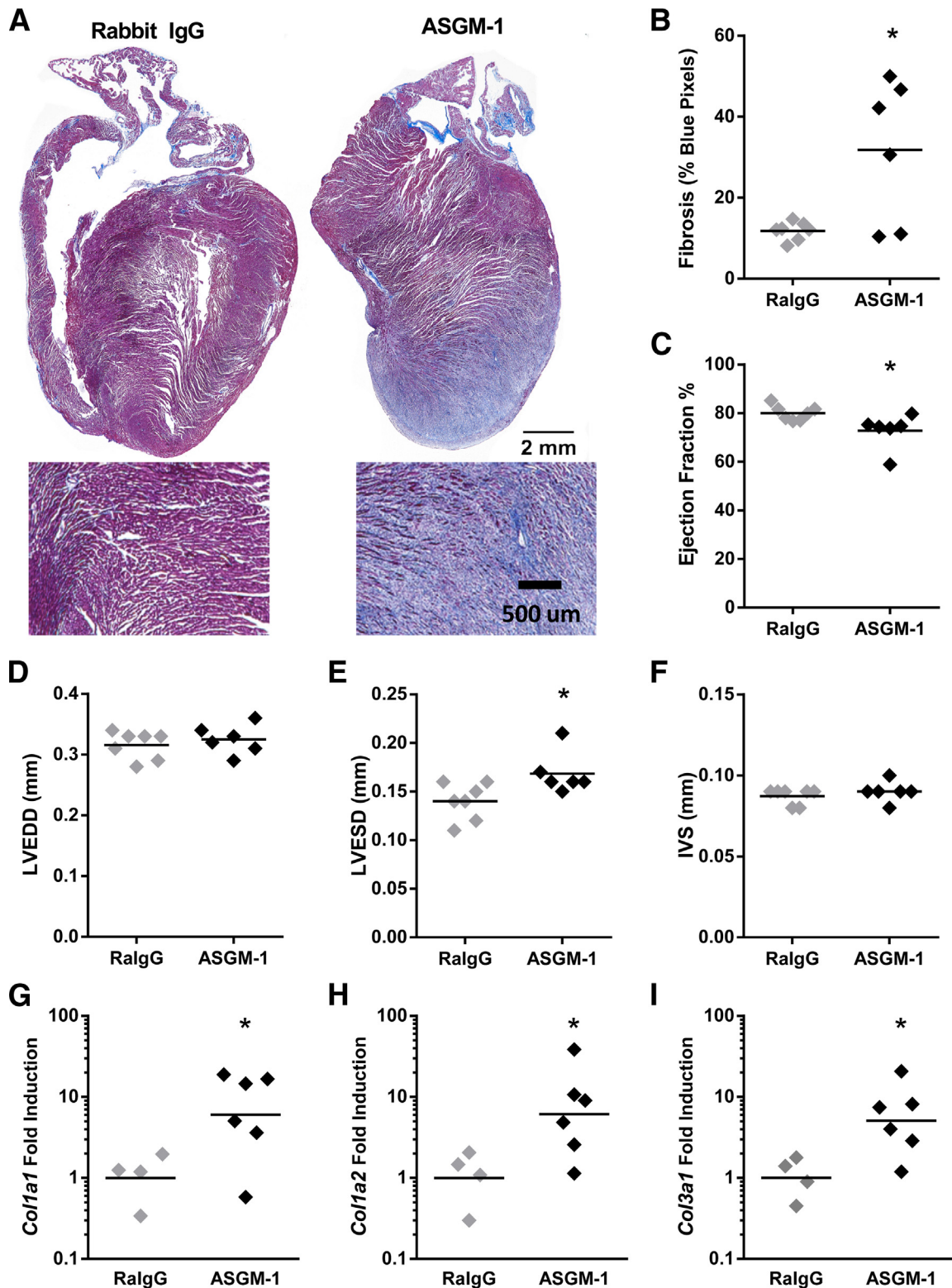
Figure 2 Depletion of natural killer cells increases collagen deposition and fibrosis during experimental autoimmune myocarditis (EAM). **A:** Representative histology of Masson's trichrome—stained cardiac sections from rabbit IgG (RaIgG) and asialogangloside GM-1 (ASGM-1)—treated animals at day 21 of EAM. **B:** Enumeration of fibrosis by calculation of red versus blue pixels on ImageJ software ($P = 0.012$). Statistics calculated by unpaired t-test. **C:** Ejection fraction ($P = 0.026$) calculated from fractional shortening and left ventricular (LV) diastole and systole. LV end diastolic dimension (LVEDD; **D**) and LV end systolic dimension (LVESD; $P = 0.03$; **E**). **F:** Intraventricular septum diameter (IVS), as measured by echocardiography. Statistics by ordinary one-way analysis of variance with post testing by Tukey's multiple-comparisons test. Collagen production as measured using real-time quantitative PCR for collagen 1a1 (Col1a1; $P = 0.04$; **G**), collagen 1a2 (Col1a2; $P = 0.03$; **H**), and collagen 3a1 (Col3a1 $P = 0.02$; **I**). Values calculated as a function of hypoxanthine-guanine phosphoribosyltransferase (HPRT) and compared against rabbit IgG. Statistics calculated by unpaired t-test. *$P < 0.05$.
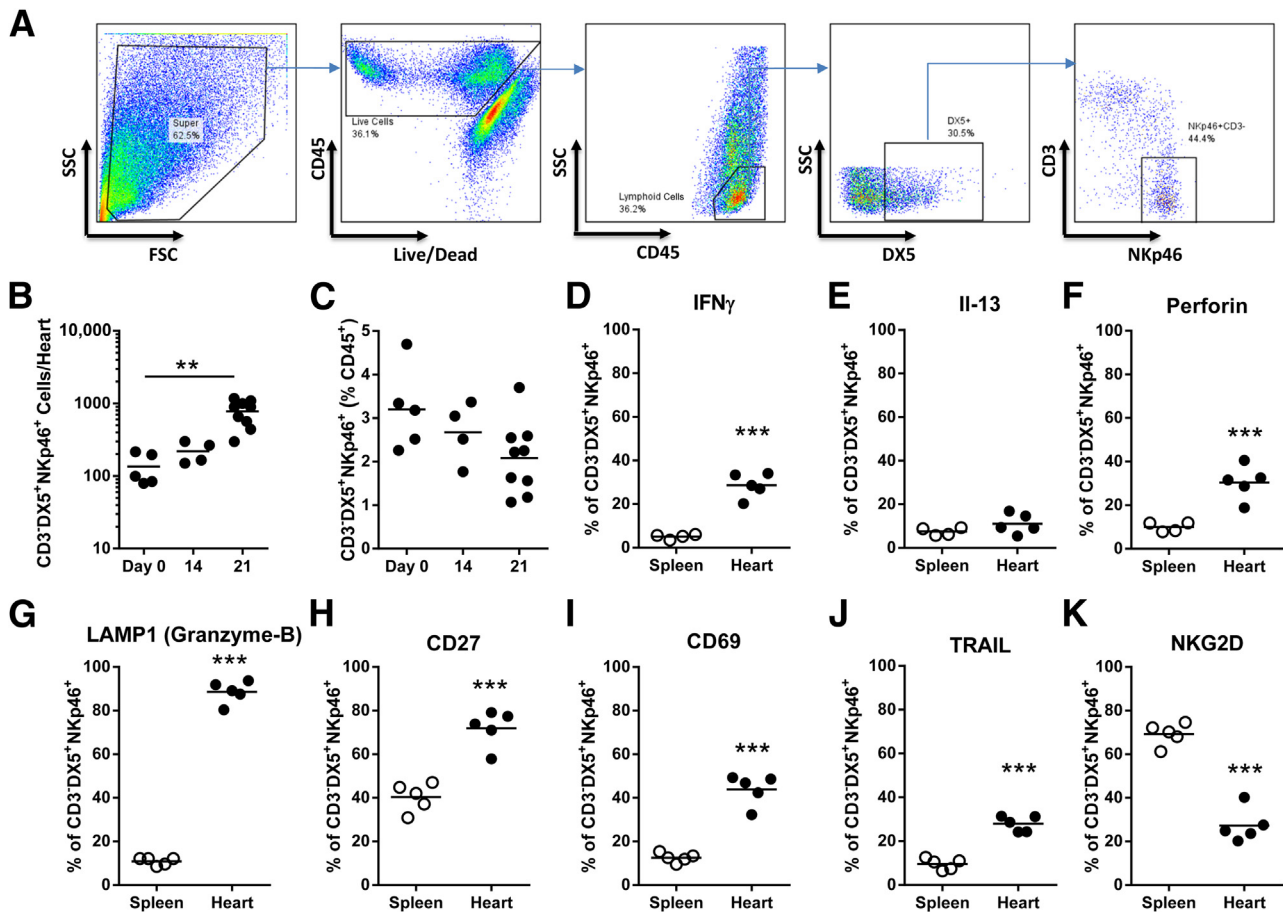
Figure 3 Activated natural killer (NK) cells accumulate in the heart during experimental autoimmune myocarditis (EAM). **A:** Gating strategy for cardiac $CD3^-DX5^+NKp46^+$ NK cells. Absolute numbers (analysis of variance $P = 0.002$; **B**) and percentages (**C**) of $CD3^-DX5^+NKp46^+$ NK cells on days 0, 14, and 21 of EAM by flow cytometry. Significance by ordinary one-way analysis of variance with post testing by Tukey's multiple-comparisons test. To determine NK physiology, cardiac and splenic $CD3^-DX5^+NKp46^+$ NK cells were stained at day 21 of EAM. Percentage of interferon γ (IFNγ; $P < 0.001$; **D**), Il-13 (**E**), and perforin ($P < 0.001$; **F**) positive cells were based on intracellular antibody staining after 4 to 6 hours of 4β-phorbol 12-myristate 13-acetate/ionomycin and Golgistop *in vitro*. **G:** Percentage of lysosomal-associated membrane protein 1 (LAMP-1$^+$), a marker for granzyme B release, staining ($P < 0.001$). Percentage of NK cells positive for activation-associated markers CD27 ($P < 0.001$; **H**), CD69 ($P < 0.001$; **I**), tumor necrosis factor—related apoptosis-inducing ligand treatment (TRAIL; $P < 0.001$; **J**), and NKG2D ($P < 0.001$; **K**). **D—F:** Significance calculated by unpaired *t*-test. **$P < 0.01$, ***$P < 0.001$. FSC, forward scatter; SSC, side scatter.

microscopy (Supplemental Figure S3C). Although NK cells induced cell death of cardiac fibroblasts, no difference was seen between untreated and activated cardiac fibroblasts (Supplemental Figure S3, D and E), indicating that NK-mediated killing of activated fibroblasts was not a likely mechanism.

NK Cells Prevent Eosinophils from Accumulating in the Heart during EAM

Given the lack of direct killing seen between NK cells and activated fibroblasts, we hypothesized that NK cells altered disease severity and fibrosis in EAM through alterations in the hematopoietic populations infiltrating the heart. Therefore, we examined changes in the cardiac infiltrate during EAM after the depletion of NK cells by flow cytometry. NK-depleted animals had increased proportion of $SSC^{hi}CD45^+$ granulocytic cells (Figure 4A). We identified that $SSC^{hi}Ly6G^{lo}SiglecF^+$ eosinophils were responsible for the increase in granulocytic cells. $SSC^{hi}Ly6G^{lo}SiglecF^+$ eosinophils increased twofold on day 14 and 10-fold on day 21 out of $CD45^+$ cells (Figure 4B). We found no changes in $SSC^{hi}Ly6G^{hi}$ neutrophils on day 14 or 21 (Figure 4C).

To determine whether the increased eosinophils in the heart seen in ASGM-1−treated mice during EAM were a cardiac-specific observation or a reflection of systemic eosinophilia in response to NK depletion, we analyzed the blood and spleens of mice depleted of NK cells during EAM at days 14 and 21. We found that, although there was a mild trend toward increased eosinophils, it was not significant (Supplemental Figure S4), underlining that the mechanism of eosinophilic control by NK cells is specific for the cardiac environment during EAM.

We also explored whether there were shifts in any other infiltrating cardiac populations during EAM. $SSC^{mid}CD11b^+$ myeloid cells, as a percentage of total $CD45^+$ cells (Supplemental Figure S5A), remained unchanged, as were $CD11b^+Ly6C^{hi}$ and $CD11b^+Ly6C^{lo}$ monocytes as a
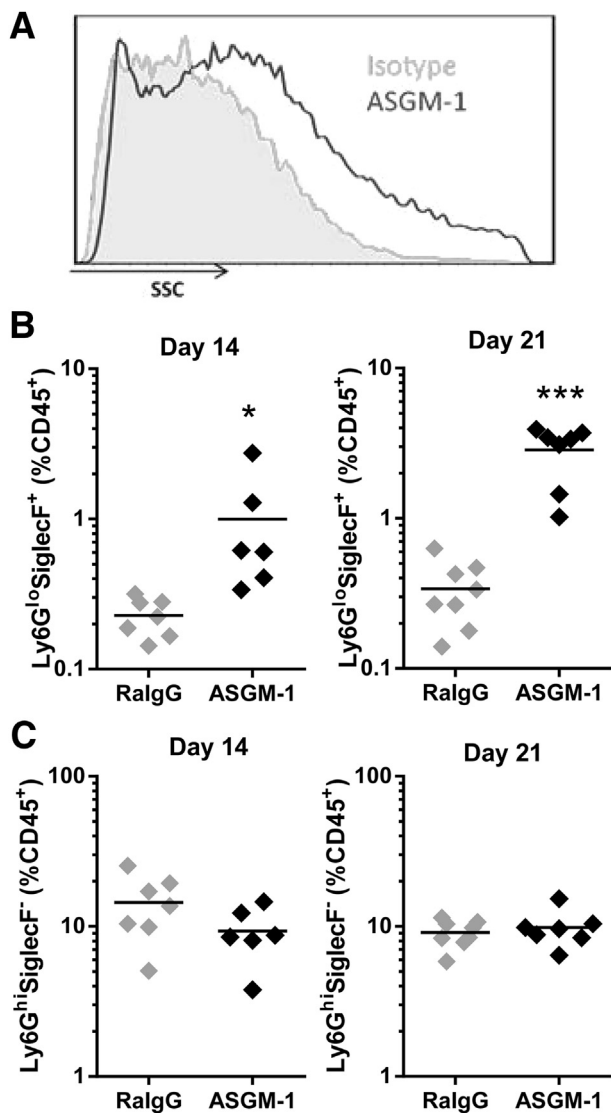
A

B

C

Figure 4 Depletion of natural killer (NK) cells increases eosinophilic infiltration in the heart. **A:** Representative side-scatter histograms of isotype and asialoganglioside GM-1 (ASGM-1) antibody treated animals at day 21. Percentage of Ly6G^{lo}SiglecF^{+} eosinophils from cardiac CD45^{+} cells on day 14 ($P = 0.043$) and day 21 ($P < 0.001$) (**B**) and SiglecF^{-}Ly6G^{hi} neutrophils at days 14 and 21 (**C**). Significance calculated by unpaired t-test. *$P < 0.05$, ***$P < 0.001$. SSC, side scatter.

proportion of total SSC^{mid}CD11b^{+} cells on day 21 (Supplemental Figure S5, B and C). The proportions of total infiltrating CD45^{+} cells of both CD11c^{hi} dendritic cells and FcϵRI$\alpha$$^{+}$cKit^{+} mast cells were also unaltered (Supplemental Figure S5, D and E). Also comparable were proportions of CD11b^{-}B220^{+} B cells and CD3^{+} and CD3^{+}CD4^{+} T cells (Supplemental Figure S5, F–H) of total CD45^{+} cells. Because EAM and eosinophil trafficking are influenced by CD4^{+} T-cell polarization,[12,28,41] we examined if NK cells affected types 1, 2, and 17 helper T cell (Th1, Th2, and Th17, respectively) populations during EAM.[12,28,37] No changes in IFN$\gamma$$^{+}$CD3^{+}CD4^{+} Th1 cells in the heart after NK depletion were found (Supplemental Figure S6A).

However, Il-13^{+} Th2 and Il-17A^{+} Th17 cells, as a fraction of total CD3^{+}CD4^{+} cells, increased at day 21, but not day 14 (Supplemental Figure S6, B and C). Thus, depletion of NK cells resulted in accumulation of eosinophils in the heart, reaching up to a 10-fold increase at the peak of inflammation, and was accompanied by a shift toward mixed Th2 and Th17 milieu in the heart.

Eosinophils in the Heart of ASGM-1—Treated Mice Have an Activated Profile

To determine whether the increased flux of eosinophils to the heart played a role in the increased disease severity, we examined the phenotype of the heart-infiltrating eosinophils for their maturation and activation status. It has been shown that mature eosinophils from the lungs of helminth-infected or the blood of asthma-induced mice have increased expression of CD11b and SiglecF protein and decreased expression of eosinophil granule—associated genes due to these granules being fully preloaded with protein.[42,43] Indeed, paraffin-embedded cardiac tissue sections of ASGM-1—treated animals with EAM showed positive staining for eosinophil granule major basic protein (Figure 5A), and cardiac eosinophils from ASGM-1—treated hearts had up-regulated levels of SiglecF and CD11b protein compared to spleen cells at day 21 (Figure 5, B and C). Consistent with this activated phenotype, cardiac eosinophils down-regulated expression of eosinophil granule—associated eosinophil peroxidase and major basic protein 2 due to their granules having already been formed during the immature stages of development (Figure 5, D and E). Cardiac eosinophils also had increased expression of Il-1b, Ccl11, and Il-6, and showed no changes in Il-4 or Il-13 expression (Figure 5, F—J). In summary, eosinophils infiltrating the heart at day 21 of ASGM-1—treated mice represent a distinct and activated population.

Eosinophils Are Necessary for Increased Myocarditis Severity in the Absence of NK Cells

To establish if the greater EAM severity in NK-depleted animals depended on the influx of activated and mature eosinophils, we depleted NK cells from eosinophil-deficient ΔdblGATA1 mice.[44] These mice have a deletion in the GATA1 promoter, leading to a specific ablation in eosinophils due to the inability of progenitors to differentiate in the bone marrow. In the absence of eosinophils, NK depletion had no effect on cardiac inflammation, as assessed from histological readings by two independent investigators using hematoxylin and eosin—stained cardiac slides at day 21 of EAM (Figure 6, A and B). In addition, we saw no increases in fibrosis evaluated by Masson's trichrome staining. In addition, cardiac function was preserved, as shown by no differences in echocardiographic parameters between NK-depleted and isotype ΔdblGATA1 groups at day 21 (Figure 6, C—G). ΔdblGATA1 mice did not respond to ASGM-1 treatment with the increased
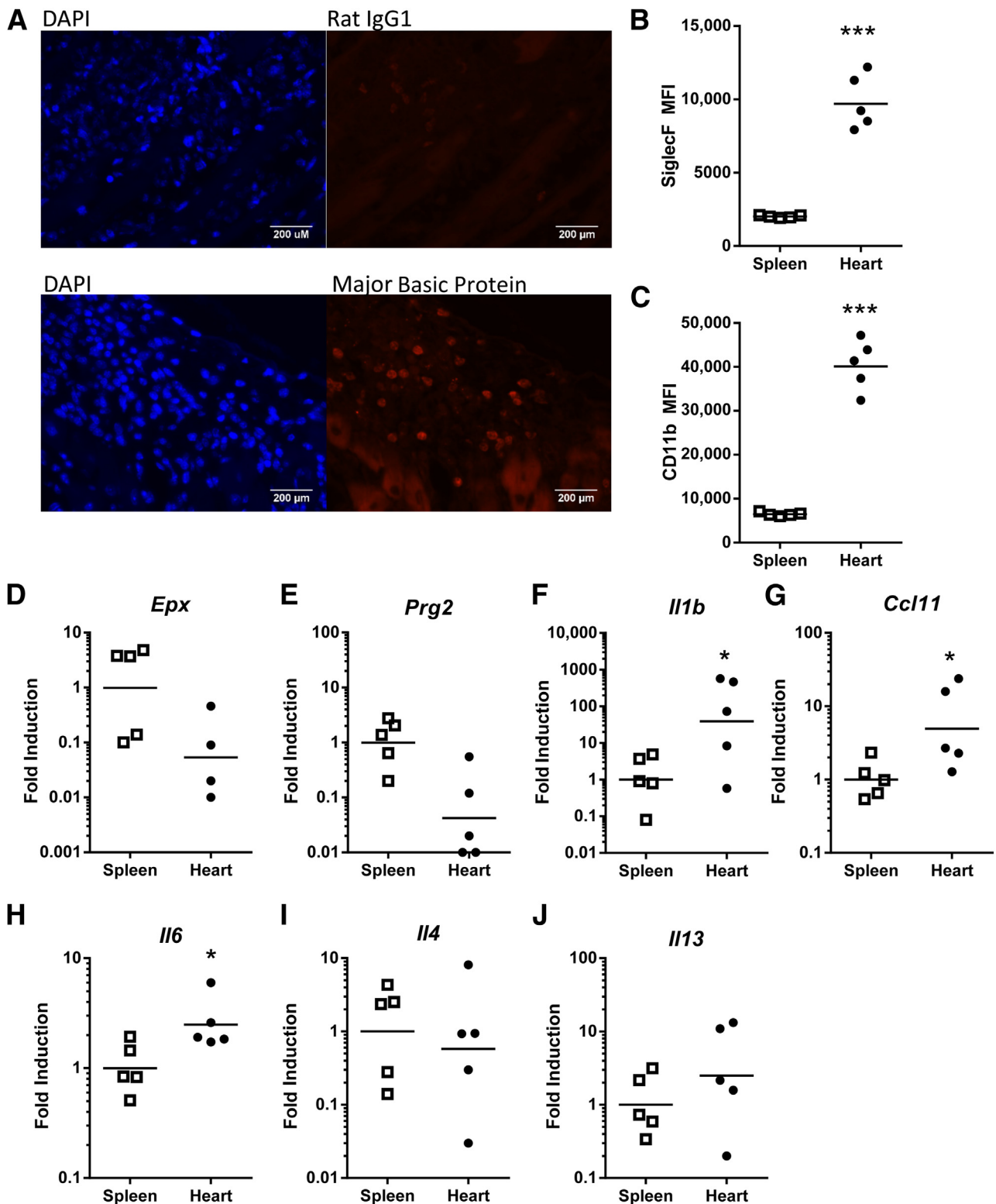
Figure 5 Activated eosinophils infiltrate the heart in the absence of natural killer cells. **A:** Immunofluorescence staining of paraffin-embedded cardiac sections from asialoganglioside GM-1 (ASGM-1)—treated mice on day 21 of experimental autoimmune myocarditis (EAM). Sections stained with 1:500 rat anti-major basic protein (MBP) primary or rat IgG antibody, 1:200 anti-rat donkey phosphatidylethanolamine (PE)—Texas Red antibody, and DAPI. Relative mean fluorescence intensity of SiglecF ($P < 0.001$; **B**) and CD11b ($P < 0.001$; **C**) on Ly6GloSiglecF$^+$ eosinophils from the heart and spleen of ASGM-1—treated animals at day 21 of EAM by flow cytometry. Levels of eosinophil peroxidase (Epx; $P = 0.05$; **D**), major basic protein 2 (Prg2; $P = 0.05$; **E**), Il1b ($P = 0.04$; **F**), chemokine ligand (Ccl) 11 ($P = 0.03$; **G**), Il6 ($P = 0.02$; **H**), Il4 (**I**), and Il13 (**J**) mRNA from fluorescence-activated cell sorted Ly6G^{lo}SiglecF^{hi} eosinophils from ASGM-1—treated mice at day 21 of EAM. Values shown as fold induction compared to spleen and controlled against hypoxanthine-guanine phosphor-ibosyltransferase (HPRT). Significance calculated by Student's t-test. *$P < 0.05$, ***$P < 0.001$. MFI, mean fluorescence intensity.
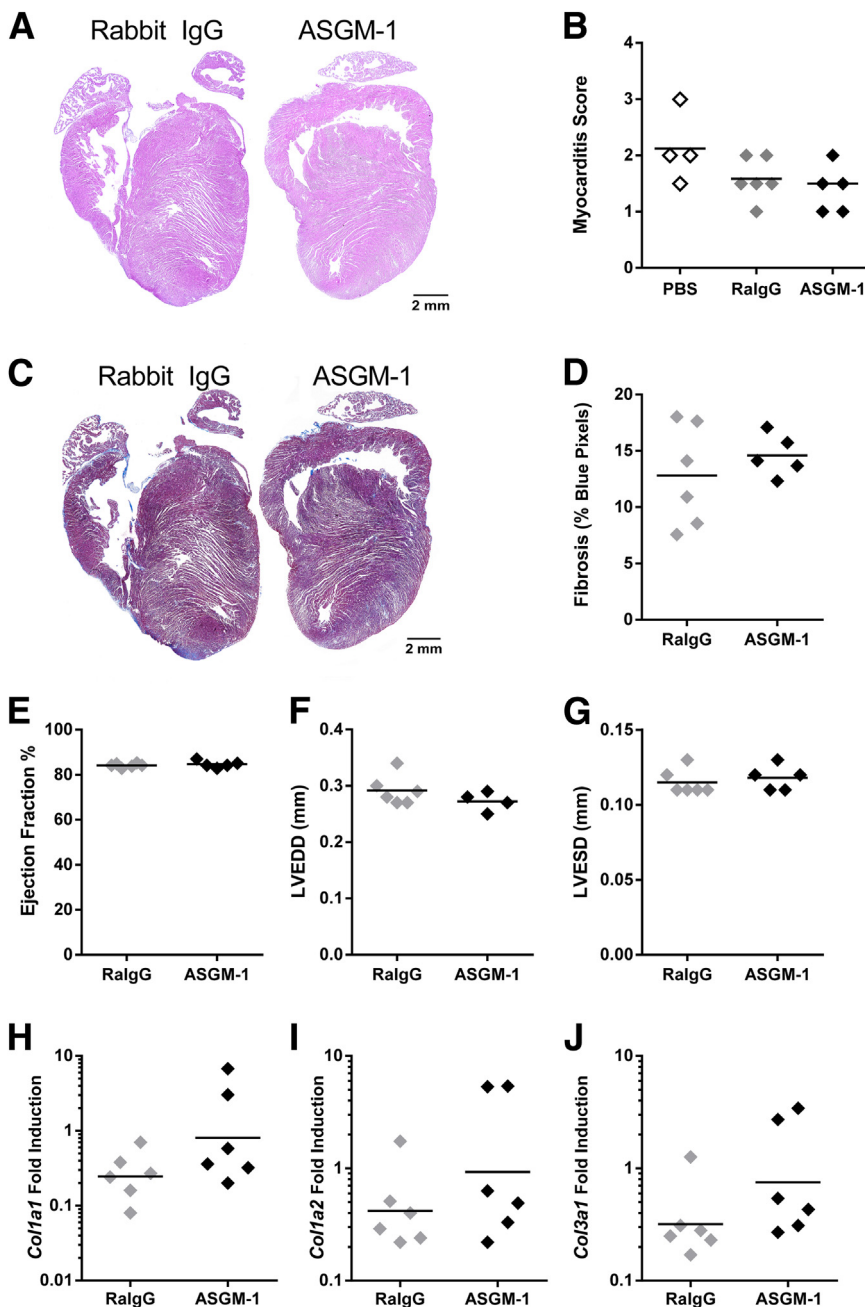
Figure 6 Eosinophil-deficient mice are phenotypically unresponsive to natural killer depletion. Representative histology from rabbit IgG (RaIgG) and asialoganglioside GM-1 (ASGM-1) antibody-treated (**A**) and scores of rabbit phosphate-buffered saline, IgG, and ASGM-1 antibody-treated ΔdblGATA1 animals (analysis of variance; **B**). Representative histology (**C**) and percentage of fibrosis (**D**) by Masson's trichrome staining of cardiac sections at day 21 of experimental autoimmune myocarditis (EAM) from rabbit IgG and ASGM-1—treated mice. Ejection fraction (**E**), left ventricular end diastolic dimension (LVEDD; **F**), and left ventricular end systolic dimension (LVESD; **G**) by echocardiography at day 21. Collagen 1 and 3 production as measured using real-time quantitative PCR for collagen 1a1 (Col1a1; **H**), collagen 1a2 (Col1a2; **I**), and collagen 3a1 (Col3a1; **J**) mRNA in hearts of rabbit IgG and ASGM-1—treated animals at day 21 of EAM. Values calculated as a function of hypoxanthine-guanine phosphoribosyltransferase (HPRT) levels and compared against rabbit IgG. Statistics calculated by unpaired t-test.

collagen 1 and 3 mRNA seen in wild-type mice (Figure 6, H—J). Therefore, myocarditis severity and cardiac fibrosis in ΔdblGATA1 mice are unaffected by NK cell depletion. This would indicate that NK cells protect the heart from eosinophilic accumulation and the subsequent development of severe myocarditis.

Ccl11 Is Involved But Not Required for the Control of Eosinophilic Infiltration by NK Cells

NK cells are not major producers of eosinophil-associated chemokines.[45–47] However, we have determined that cardiac fibroblasts are an active source of cytokines and chemokines and can control the types of immune cells infiltrating the heart during myocarditis.[48] Eotaxins are prominent modulators of eosinophil trafficking and accumulation. In EAM, the depletion of NK cells increased eotaxin expression in whole heart tissue (Figure 7A) and isolated cardiac fibroblasts on day 21 of EAM (Figure 7, A—C), as seen by qPCR. To examine if NK cells affected eotaxin production *in vitro*, we co-cultured naïve adult cardiac fibroblasts and NK cells for 96 hours. NK cells suppressed Il-4—mediated Ccl11 (Figure 7D) and increased IP-10 (Cxcl10), a negative eosinophil regulator, produced by cardiac fibroblasts (Supplemental Figure S7A). Down-regulation of monocyte chemoattractant protein-1 (Ccl2),
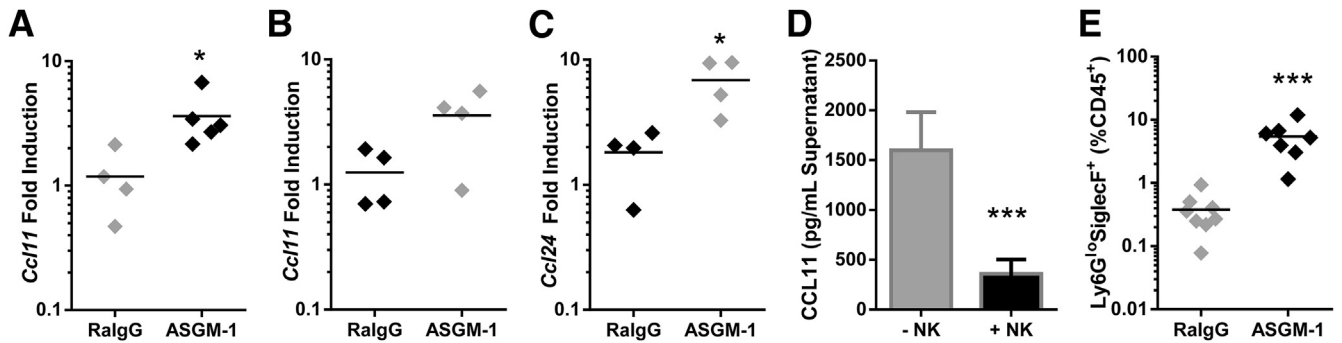
Figure 7 Chemokine ligand (Ccl) 11 is involved, but not required, for the suppression of eosinophils by natural killer (NK) cells. Ccl11 mRNA at day 21 of experimental autoimmune myocarditis (EAM) in whole heart ($P = 0.004$; **A**) and isolated cardiac fibroblasts of rabbit IgG and asialoganglioside GM-1 (ASGM-1)—treated animals (**B**). **C:** CCL24 mRNA in isolated cardiac fibroblasts of rabbit IgG (RaIgG) and ASGM-1—treated animals at day 21 of EAM. **D:** Ccl11 in the supernatant after a 96-hour culture of wild-type cardiac fibroblasts with or without NK cells ($P < 0.001$). **E:** Percentage of Ly6G^{lo}SiglecF^{+} eosinophils at day 21 of EAM in rabbit IgG and ASGM-1—treated $Ccr3^{-/-}$ animals. Significance by Student's t-test. $*P < 0.05$, $***P < 0.001$.

macrophage inflammatory protein-1β (Ccl4), regulated on activation normal T cell expressed and secreted (Ccl5), and keratinocyte chemoattractant (Cxcl1) (Supplemental Figure S7, B—E) also occurred in the presence of NK cells. In response to Il-4, cardiac fibroblasts produced Il-5, but were unresponsive to NK cells (Supplemental Figure S7F).

To address whether NK suppression of eotaxins would be sufficient to prevent eosinophil accumulation, we used mice deficient in Ccr3, the sole receptor of Ccl11 and Ccl24.[49] Depletion of NK cells in $Ccr3^{-/-}$ mice still resulted in the influx of eosinophils into the heart during EAM (Figure 7E), indicating that NK cells do not control eosinophils through only eotaxins and that other eosinophilic chemokines are able to drive eosinophil trafficking in the absence of NK cells. Thus, Ccl11 is involved, but not required, for the control of eosinophilic infiltration in the heart by NK cells.

Ifnγ and Cxcl9 Are Not Required by NK Cells to Control Eosinophilic Infiltration

During EAM, IFNγ was significantly up-regulated in cardiac NK cells accumulating in the heart. Monokine induced by interferon-γ (Cxcl9), a major negative regulator of eosinophil trafficking, is directly controlled by Ifnγ. We determined that in ASGM-1—treated mice, expression of Cxcl9 was decreased compared to the isotype control groups at day 21 of EAM (Supplemental Figure S8A), and that similar to Cxcl10 (Supplemental Figure S7A), the presence of NK cells in culture with primary cardiac fibroblasts significantly increased levels of Cxcl9 in the supernatant (Supplemental Figure S8B). In addition, our data indicate that Ifnγ produced by NK cells is absolutely required for Cxcl9 production being instigated, because Ifnγ receptor—deficient (IFNγR1$^{-/-}$) cardiac fibroblasts were unresponsive to the presence of NK cells (Supplemental Figure S8C). These findings were consistent *in vivo*, because we observed significant decreases in the protein levels of Cxcl9 in the hearts of IFNγ$^{-/-}$ animals at day 14 of EAM (Supplemental

Figure S8D). By using IFNγ$^{-/-}$ mice to model the effects of diminished Cxcl9 and the absence of NK-sourced Ifnγ, we depleted NK cells in IFNγ$^{-/-}$ mice and examined eosinophilic accumulation in the heart on day 21. Similar to the $Ccr3^{-/-}$ mice, IFNγ$^{-/-}$ mice still continued to accumulate significantly more eosinophils in the heart (Supplemental Figure S8E). In conclusion, both Cxcl9 and IFNγ may contribute to the NK-mediated control of eosinophils in the heart, but they are not required.

NK Cells Directly Induce Apoptosis of Eosinophils

Finally, we examined whether NK cells could inhibit eosinophil infiltration through direct interactions between the two cell types. Recent studies showed that human NK cells induce activation and apoptosis of eosinophils.[50,51] We explored this as one avenue of NK-mediated control of eosinophil accumulation in the heart during cardiac inflammation. NK cells and eosinophils were negatively sorted from naïve $Rag1^{-/-}$ spleens and Cd3δ—IL-5—transgenic (NJ.1638) blood, respectively, and co-cultured for 3 hours at 5:1 and 10:1 ratios. Compared to eosinophils alone, NK cells induced apoptosis, but not degranulation, as measured by side scatter, of eosinophils in a dose-dependent manner (Figure 8A). At this 3-hour time point, early apoptosis was measurable using annexin V, but no changes were yet seen with a viability dye measured through cell permeabilization (Figure 8, B and C). NK cells did not induce eosinophil activation either, as shown by changes in levels of SiglecF and CD11b, unlike reports in human cells (Figure 8, D and E).[51] In summary, we show that, similarly to human NK cells, mice NK cells cause apoptosis of eosinophils.

Discussion

Previous studies[13,14] have demonstrated that NK cells limit disease severity in CB3- and mouse cytomegalovirus—induced myocarditis by suppressing virus replication. In
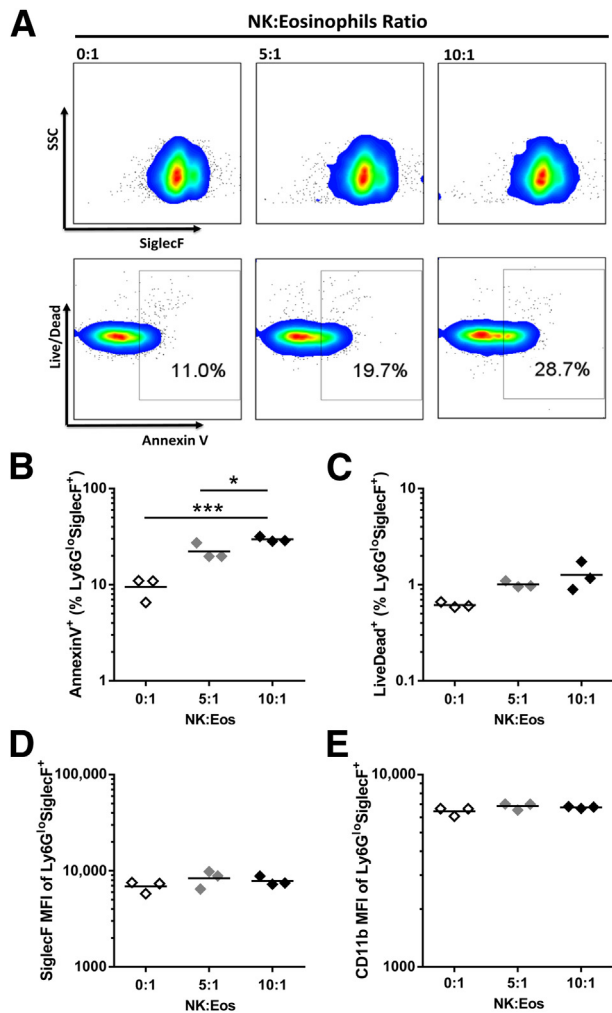
Figure 8 Natural killer (NK) cells induce apoptosis in eosinophils (Eos) *in vitro*. **A:** Representative side scatter versus SiglecF and LIVE/DEAD viability dye versus annexin V plots of Ly6G^{lo}SiglecF$^+$ eosinophils after a 3-hours co-culture with primary naïve NK cells. Percentage of annexin V—positive (analysis of variance $P < 0.001$; **B**) and LIVE/DEAD stain—positive Ly6G^{lo}SiglecF$^+$ eosinophils (**C**). Average mean fluorescence intensity of activation markers SiglecF (**D**) and CD11b (**E**) of Ly6G^{lo}SiglecF^{hi} eosinophils. Statistics calculated by one-way analysis of variance with post testing by Tukey's test. *$P < 0.05$, ***$P < 0.001$. SSC, side scatter.

addition, we showed that depletion of NK cells rendered previously resistant strains of mice susceptible to viral myocarditis.[13] Herein, we demonstrate that the protective qualities of NK cells extend beyond viral inhibition. Activated NK cells accumulated in the heart throughout EAM and actively suppressed autoimmune-mediated inflammation, because the depletion of NK cells during EAM led to increased cardiac inflammation and fibrosis. This was caused primarily by a 10-fold increase in the proportion of eosinophils in the cardiac infiltrate, because eosinophil-deficient ΔdblGATA1 animals did not display increased myocarditis severity in response to NK cell depletion. Furthermore, this increase of eosinophils was specific for the cardiac environment and was not found in the periphery during EAM. On the basis of these data, we conclude that

NK cells limited eosinophil accumulation in the heart during EAM and in the absence of NK cells, increases in eosinophils drove the amplified disease severity.

Similar to studies in RA patients, we showed that NK cells occupying local sites of autoimmune-mediated inflammation have a distinct and activated phenotype compared to those in the periphery.[20,22] Cardiac NK cells up-regulated CD27, tumor necrosis factor—related apoptosis-inducing ligand treatment, and CD69 on their cell surfaces, but down-regulated NKG2D. The down-regulation of NKG2D is surprising because nonobese diabetes can be prevented with anti-NKG2D antibodies and NKG2D$^+$ cells are correlated with clinical Crohn's and RA severity.[52—54] However, total NKG2D in these studies was targeted, including those expressed on NK T and δγ T cells.[55] Therefore, the role of NKG2D on NK cells is undetermined and its down-regulation in EAM indicates it may have a minimal role in autoimmunity.

Our finding that eosinophils promote severe cardiac inflammation is supported by other reports of eosinophils driving myocarditis severity. In CB3-induced myocarditis, infiltrating eosinophils significantly increased disease. Soluble ST2, an Il-33 receptor decoy, prevented eosinophilia and reduced myocarditis without altering viral burden.[56] Similarly, IFNγ$^{-/-}$Il17A$^{-/-}$ mice display massively inflamed hearts and up to 50% fatality by day 21 of EAM, a phenotype that is reversed in the absence of eosinophils by crossing these animals to dblGATA1 mice.[57]

Although the numbers of eosinophils infiltrating the heart after NK cell depletion (10% to 15%) during EAM do not approach clinical or animal models of eosinophilic myocarditis (up to 50%), we clearly demonstrate that even this moderate increase has significant consequences on disease outcome.[56,57] Clinically, infiltrating eosinophils are found in severe giant cell myocarditis and these patients, along with necrotizing eosinophilic myocarditis, have poor clinical prognosis.[58,59] Other clinical entities in which moderate levels of eosinophils are found infiltrating the myocardium include hypersensitivity and drug reactions, parasitic infections, vasculitis and granulomatous diseases, and idiopathic hypereosinophilic syndrome.[60] Little is known about the cardiac eosinophil profile; however, in all cases, cardiac necrosis, thrombosis, and fibrosis are found.[61]

We found that eosinophils in the hearts of ASGM-1—treated animals displayed a mature, activated profile with fully formed granules containing cationic proteins. Cardiac tissue stained positive for major basic protein by immunofluorescence. qPCR results showed the down-regulation of eosinophil peroxidase and major basic protein mRNA in eosinophils isolated from the heart versus the spleen at day 21 of EAM, indicating that the active transcription of these proteins, characteristic of immature eosinophils, was no longer taking place. Mature eosinophils contain fully formed granules of these cationic proteins to be released instantly on specific activation and, therefore, have no need for further transcription of these genes.[43] Furthermore, their

up-regulation of SiglecF and CD11b is consistent with activated lung eosinophils from *Nippostrongylus brasiliensis*−infected mice.[42,50] This up-regulation of activation markers cannot be attributed to the collagenase treatment implemented for cardiac dissociation because we have found the treatment with collagenase does not alter cell phenotypes (data not shown). Cardiac eosinophils did not up-regulate Il-4 and Il-13, despite reports that eosinophils can regulate muscle repair through Il-4 and Il-13.[62] However, cardiac eosinophils significantly up-regulated Il-6 and Tgf-β, mirroring activated eosinophils in airway inflammation and fibrosis models.[50,63−65] These cytokines are involved in multiple fibrosis pathways and may be responsible for the eosinophil-mediated fibrosis seen in ASGM-1−treated wild-type mice.

An alternative hypothesis for the regulation of disease severity by NK cells through eosinophils involves alterations in monocytes. Monocytes, as the majority of cardiac infiltrating cells during EAM, can alter disease severity.[33,48] We have shown that monocyte control of disease was due to alterations in Th17 cells.[33,34,41,66] However, the increased disease in the absence of NK cells was not accompanied by changes in SSC^{mid}CD11b$^+$ monocytes or the Ly6C^{hi} inflammatory monocyte subpopulation. Furthermore, although we did see increases in Th2 and Th17 populations, these shifts occurred after increases in eosinophilic infiltration and are likely symptomatic, as opposed to causative, of these changes. Therefore, we do not believe that NK cells protect against autoimmune-mediated inflammation through the regulation of monocytic or T-cell populations.

To investigate how NK cells prevent eosinophils from accumulating in the heart during myocarditis, we turned our attention to interactions between cardiac fibroblasts and NK cells. Studies have shown that tumor fibroblasts interfere with NK cell cytotoxicity, and synoviocytes in RA express NK-receptor ligands that result in NK cell activation.[67,68] However, we did not find that NK cells targeted activated cardiac fibroblasts for killing, unlike studies in liver fibrosis.[39,40,69] Our group recently showed that Il-17A−stimulated cardiac fibroblasts produce key chemokines and cytokines that are critical downstream effectors in recruiting and differentiating myeloid cells.[48,70] We suspect that cardiac fibroblasts secrete unique profiles of cytokines and chemokines when exposed to a different cytokine milieu or on interaction with immune cells in the heart. Indeed, we showed that NK cells controlled chemokine profiles secreted by cardiac fibroblasts during EAM. On depletion of NK cells, cardiac fibroblast−derived chemokines generated a pro-eosinophilic environment *in vivo*, *in vitro*, and *ex vivo*.

Of these chemokines, eotaxins and CXCL9, major controllers of eosinophilic trafficking in asthma and allergy, were the most dysregulated.[71−74] We were able to show that CXCL9 was directly controlled by NK-derived IFNγ and that in the absence of IFNγ, CXCL9 levels were diminished. However, most chemokines are notorious for functional redundancy and it is difficult to obtain phenotypic evidence

for their role in disease.[75,76] Ccl11 and CXCL9 are no exception to this rule. This was supported by the failure of Ccr3$^{-/-}$ and IFNγ$^{-/-}$ mice to show any changes in eosinophilic accumulation in the absence of NK cells. Furthermore, although this relationship between NK cells and resident cardiac fibroblasts was undeniably present in EAM, it may not be the predominant manner in which NK cells control eosinophilic infiltration.

Therefore, we explored whether NK cells could directly inhibit eosinophils, by either deactivation or killing. Reports in human cells indicated that the co-culture of NK cells with naïve eosinophils resulted in eosinophil activation and degranulation.[77,78] By annexin V staining, a marker of early apoptosis, we show that NK cells induce apoptosis of eosinophils *in vitro*. Delayed apoptosis of eosinophils has been implicated in multiple asthma models, and the induction of apoptosis by pharmacological agents contributes to the clearance of disease.[79−81] Therefore, the increased eosinophil numbers seen in the absence of NK cells may be the result of a deficiency in apoptotic signals during cardiac inflammation.

These data open the possibility for NK cells or their products as a biological therapy for myocarditis. NK-related therapies are an area of avid cancer research, and the same resources could be used to treat autoimmune disorders.[82−84] Developments in the treatment for clinical myocarditis are constricted by the opposing needs in the viral and autoimmune components of disease. Ideally, an intervention could be designed that would target both needs simultaneously. Our laboratory has now shown that NK cells are clearly protective in both viral and autoimmune-mediated driven forms of myocarditis. In essence, NK cells or NK-derived products concurrently could serve as an antiviral therapy and also as an immunosuppressant.

Acknowledgment

Supplemental Data

Supplemental material for this article can be found at *http://dx.doi.org/10.1016/j.ajpath.2014.11.023*.

References

1. Andreoletti L, Leveque N, Boulagnon C, Brasselet C, Fornes P: Viral causes of human myocarditis. Arch Cardiovasc Dis 2009, 102: 559−568
2. Cihakova D, Rose NR: Pathogenesis of myocarditis and dilated cardiomyopathy. Adv Immunol 2008, 99:95−114
3. Rose NR, Cihakova D: Cardiomyopathies. Autoimmunity 2004, 37: 347−350
4. Seshadri S, Narula J, Chopra P: Asymptomatic eosinophilic myocarditis: 2 + 2 = 4 or 5! Int J Cardiol 1991, 31:348−349

5. Huston B, Froloff V, Mills K, McGee M: Death due to eosinophilic necrotizing myocarditis despite steroid treatment. Am J Forensic Med Pathol 2013, 34:95−97

6. Baandrup U: Eosinophilic myocarditis. Herz 2012, 37:849−852

7. Al Ali AM, Straatman LP, Allard MF, Ignaszewski AP: Eosinophilic myocarditis: case series and review of literature. Can J Cardiol 2006, 22:1233−1237

8. Carniel E, Sinagra G, Bussani R, Di Lenarda A, Pinamonti B, Lardieri G, Silvestri F: Fatal myocarditis: morphologic and clinical features. Ital Heart J 2004, 5:702−706

9. Cooper LT, Baughman KL, Feldman AM, Frustaci A, Jessup M, Kuhl U, Levine GN, Narula J, Starling RC, Towbin J, Virmani R: The role of endomyocardial biopsy in the management of cardiovascular disease: a scientific statement from the American Heart Association, the American College of Cardiology, and the European Society of Cardiology. Endorsed by the Heart Failure Society of America and the Heart Failure Association of the European Society of Cardiology. J Am Coll Cardiol 2007, 50:1914−1931

10. Wensky AK, Furtado GC, Marcondes MC, Chen S, Manfra D, Lira SA, Zagzag D, Lafaille JJ: IFN-gamma determines distinct clinical outcomes in autoimmune encephalomyelitis. J Immunol 2005, 174:1416−1423

11. Al-Haddad S, Riddell RH: The role of eosinophils in inflammatory bowel disease. Gut 2005, 54:1674−1675

12. Kay AB: The role of eosinophils in the pathogenesis of asthma. Trends Mol Med 2005, 11:148−152

13. Fairweather D, Kaya Z, Shellam GR, Lawson CM, Rose NR: From infection to autoimmunity. J Autoimmun 2001, 16:175−186

14. Godeny EK, Gauntt CJ: Involvement of natural killer cells in coxsackievirus B3-induced murine myocarditis. J Immunol 1986, 137: 1695−1702

15. Loh J, Chu DT, O'Guin AK, Yokoyama WM, Virgin HW: Natural killer cells utilize both perforin and gamma interferon to regulate murine cytomegalovirus infection in the spleen and liver. J Virol 2005, 79:661−667

16. Johansson S, Berg L, Hall H, Hoglund P: NK cells: elusive players in autoimmunity. Trends Immunol 2005, 26:613−618

17. Perricone R, Perricone C, De Carolis C, Shoenfeld Y: NK cells in autoimmunity: a two-edg'd weapon of the immune system. Autoimmun Rev 2008, 7:384−390

18. Santiago-Schwarz F, Kay C, Panagiotopoulos C, Carsons SE: Rheumatoid arthritis serum or synovial fluid and interleukin 2 abnormally expand natural killer-like cells that are potent stimulators of IgM rheumatoid factor. J Rheumatol 1992, 19:223−228

19. Pridgeon C, Lennon GP, Pazmany L, Thompson RN, Christmas SE, Moots RJ: Natural killer cells in the synovial fluid of rheumatoid arthritis patients exhibit a CD56bright,CD94bright,CD158negative phenotype. Rheumatology (Oxford) 2003, 42:870−878

20. Dalbeth N, Gundle R, Davies RJ, Lee YC, McMichael AJ, Callan MF: CD56bright NK cells are enriched at inflammatory sites and can engage with monocytes in a reciprocal program of activation. J Immunol 2004, 173:6418−6426

21. Ren J, Feng Z, Lv Z, Chen X, Li J: Natural killer-22 cells in the synovial fluid of patients with rheumatoid arthritis are an innate source of interleukin 22 and tumor necrosis factor-alpha. J Rheumatol 2011, 38:2112−2118

22. Dalbeth N, Callan MF: A subset of natural killer cells is greatly expanded within inflamed joints. Arthritis Rheum 2002, 46: 1763−1772

23. Shi FD, Takeda K, Akira S, Sarvetnick N, Ljunggren HG: IL-18 directs autoreactive T cells and promotes autodestruction in the central nervous system via induction of IFN-gamma by NK cells. J Immunol 2000, 165:3099−3104

24. Yang YZ, Jin PY, Wang QD: [Natural killer cell activity and induction of alpha and gamma interferon in patients with Coxsackie B viral myocarditis] Chinese. Zhonghua Xin Xue Guan Bing Za Zhi 1988, 16:337−339, 382

25. Kanda T, Ohshima S, Yuasa K, Watanabe T, Suzuki T, Murata K: Idiopathic myocarditis associated with T-cell subset changes and depressed natural killer activity. Jpn Heart J 1990, 31:741−744

26. Chow LH, Ye Y, Linder J, McManus BM: Phenotypic analysis of infiltrating cells in human myocarditis: an immunohistochemical study in paraffin-embedded tissue. Arch Pathol Lab Med 1989, 113: 1357−1362

27. Takahashi K, Aranami T, Endoh M, Miyake S, Yamamura T: The regulatory role of natural killer cells in multiple sclerosis. Brain 2004, 127:1917−1927

28. Afanasyeva M, Georgakopoulos D, Rose NR: Autoimmune myocarditis: cellular mediators of cardiac dysfunction. Autoimmun Rev 2004, 3:476−486

29. Cihakova D, Sharma RB, Fairweather D, Afanasyeva M, Rose NR: Animal models for autoimmune myocarditis and autoimmune thyroiditis. Methods Mol Med 2004, 102:175−193

30. Neu N, Beisel KW, Traystman MD, Rose NR, Craig SW: Autoantibodies specific for the cardiac myosin isoform are found in mice susceptible to Coxsackievirus B3-induced myocarditis. J Immunol 1987, 138:2488−2492

31. Rose NR: The significance of autoimmunity in myocarditis. Ernst Schering Res Found Workshop 2006, (55):141−154

32. Baldeviano GC, Barin JG, Talor MV, Srinivasan S, Bedja D, Zheng D, Gabrielson K, Iwakura Y, Rose NR, Cihakova D: Interleukin-17A is dispensable for myocarditis but essential for the progression to dilated cardiomyopathy. Circ Res 2010, 106: 1646−1655

33. Barin JG, Baldeviano GC, Talor MV, Wu L, Ong S, Quader F, Chen P, Zheng D, Caturegli P, Rose NR, Cihakova D: Macrophages participate in IL-17-mediated inflammation. Eur J Immunol 2012, 42: 726−736

34. Barin JG, Talor MV, Baldeviano GC, Kimura M, Rose NR, Cihakova D: Mechanisms of IFNgamma regulation of autoimmune myocarditis. Exp Mol Pathol 2010, 89:83−91

35. Cihakova D, Barin JG, Afanasyeva M, Kimura M, Fairweather D, Berg M, Talor MV, Baldeviano GC, Frisancho S, Gabrielson K, Bedja D, Rose NR: Interleukin-13 protects against experimental autoimmune myocarditis by regulating macrophage differentiation. Am J Pathol 2008, 172:1195−1208

36. Kasai M, Yoneda T, Habu S, Maruyama Y, Okumura K, Tokunaga T: In vivo effect of anti-asialo GM1 antibody on natural killer activity. Nature 1981, 291:334−335

37. Habu S, Fukui H, Shimamura K, Kasai M, Nagai Y, Okumura K, Tamaoki N: In vivo effects of anti-asialo GM1, I: reduction of NK activity and enhancement of transplanted tumor growth in nude mice. J Immunol 1981, 127:34−38

38. O'Connell TD, Rodrigo MC, Simpson PC: Isolation and culture of adult mouse cardiac myocytes. Methods Mol Biol 2007, 357: 271−296

39. Gonzalez A, Katz JD, Mattei MG, Kikutani H, Benoist C, Mathis D: Genetic control of diabetes progression. Immunity 1997, 7:873−883

40. Poirot L, Benoist C, Mathis D: Natural killer cells distinguish innocuous and destructive forms of pancreatic islet autoimmunity. Proc Natl Acad Sci U S A 2004, 101:8102−8107

41. Barin JG, Cihakova D: Control of inflammatory heart disease by CD4+ T cells. Ann N Y Acad Sci 2013, 1285:80−96

42. Johansson MW: Activation states of blood eosinophils in asthma. Clin Exp Allergy 2014, 44:482−498

43. Voehringer D, van Rooijen N, Locksley RM: Eosinophils develop in distinct stages and are recruited to peripheral sites by alternatively activated macrophages. J Leukoc Biol 2007, 81:1434−1444

44. Yu C, Cantor AB, Yang H, Browne C, Wells RA, Fujiwara Y, Orkin SH: Targeted deletion of a high-affinity GATA-binding site in the GATA-1 promoter leads to selective loss of the eosinophil lineage in vivo. J Exp Med 2002, 195:1387−1395

45. Lanier LL: Activating and inhibitory NK cell receptors. Adv Exp Med Biol 1998, 452:13−18

46. Lanier LL: NK cell recognition. Annu Rev Immunol 2005, 23: 225−274
47. Vivier E, Tomasello E, Baratin M, Walzer T, Ugolini S: Functions of natural killer cells. Nat Immunol 2008, 9:503−510
48. Wu L, Ong S, Talor MV, Barin JG, Baldeviano GC, Kass DA, Bedja D, Zhang H, Sheikh A, Margolick JA, Iwakura Y, Rose NR, Cihakova D: Cardiac fibroblasts mediate IL-17A-driven inflammatory dilated cardiomyopathy. J Exp Med 2014, 211:1449−1464
49. Xanthou G, Duchesnes CE, Williams TJ, Pease JE: CCR3 functional responses are regulated by both CXCR3 and its ligands CXCL9, CXCL10 and CXCL11. Eur J Immunol 2003, 33: 2241−2250
50. Barnig C, Cernadas M, Dutile S, Liu X, Perrella MA, Kazani S, Wechsler ME, Israel E, Levy BD: Lipoxin A4 regulates natural killer cell and type 2 innate lymphoid cell activation in asthma. Sci Transl Med 2013, 5:174ra126
51. Awad A, Yassine H, Barrier M, Vorng H, Marquillies P, Tsicopoulos A, Duez C: Natural killer cells induce eosinophil activation and apoptosis. PLoS One 2014, 9:e94492
52. Sungur CM, Tang-Feldman YJ, Zamora AE, Alvarez M, Pomeroy C, Murphy WJ: Murine NK-cell licensing is reflective of donor MHC-I following allogeneic hematopoietic stem cell transplantation in murine cytomegalovirus responses. Blood 2013, 122: 1518−1521
53. Zhang B, Yamamura T, Kondo T, Fujiwara M, Tabira T: Regulation of experimental autoimmune encephalomyelitis by natural killer (NK) cells. J Exp Med 1997, 186:1677−1687
54. Lassen MG, Lukens JR, Dolina JS, Brown MG, Hahn YS: Intrahepatic IL-10 maintains NKG2A+Ly49- liver NK cells in a functionally hyporesponsive state. J Immunol 2010, 184:2693−2701
55. Fathman JW, Bhattacharya D, Inlay MA, Seita J, Karsunky H, Weissman IL: Identification of the earliest natural killer cell-committed progenitor in murine bone marrow. Blood 2011, 118: 5439−5447
56. Abston ED, Barin JG, Cihakova D, Bucek A, Coronado MJ, Brandt JE, Bedja D, Kim JB, Georgakopoulos D, Gabrielson KL, Mitzner W, Fairweather D: IL-33 independently induces eosinophilic pericarditis and cardiac dilation: ST2 improves cardiac function. Circ Heart Fail 2012, 5:366−375
57. Barin JG, Baldeviano GC, Talor MV, Wu L, Ong S, Fairweather D, Bedja D, Stickel NR, Fontes JA, Cardamone AB, Zheng D, Gabrielson KL, Rose NR, Cihakova D: Fatal eosinophilic myocarditis develops in the absence of IFN-gamma and IL-17A. J Immunol 2013, 191:4038−4047
58. Hyogo M, Kamitani T, Oguni A, Kawasaki S, Miyanaga H, Takahashi T, Kunishige H, Andachi H: Acute necrotizing eosinophilic myocarditis with giant cell infiltration after remission of idiopathic thrombocytopenic purpura. Intern Med 1997, 36:894−897
59. Litovsky SH, Burke AP, Virmani R: Giant cell myocarditis: an entity distinct from sarcoidosis characterized by multiphasic myocyte destruction by cytotoxic T cells and histiocytic giant cells. Mod Pathol 1996, 9:1126−1134
60. Rezaizadeh H, Sanchez-Ross M, Kaluski E, Klapholz M, Haider B, Gerula C: Acute eosinophilic myocarditis: diagnosis and treatment. Acute Card Care 2010, 12:31−36
61. Weller PF, Bubley GJ: The idiopathic hypereosinophilic syndrome. Blood 1994, 83:2759−2779
62. Heredia JE, Mukundan L, Chen FM, Mueller AA, Deo RC, Locksley RM, Rando TA, Chawla A: Type 2 innate signals stimulate fibro/adipogenic progenitors to facilitate muscle regeneration. Cell 2013, 153:376−388
63. Louch WE, Sheehan KA, Wolska BM: Methods in cardiomyocyte isolation, culture, and gene transfer. J Mol Cell Cardiol 2011, 51: 288−298
64. Lim YC, Luscinskas FW: Isolation and culture of murine heart and lung endothelial cells for in vitro model systems. Methods Mol Biol 2006, 341:141−154
65. Afanasyeva M, Georgakopoulos D, Belardi DF, Ramsundar AC, Barin JG, Kass DA, Rose NR: Quantitative analysis of myocardial inflammation by flow cytometry in murine autoimmune myocarditis: correlation with cardiac function. Am J Pathol 2004, 164:807−815
66. Barin JG, Rose NR, Cihakova D: Macrophage diversity in cardiac inflammation: a review. Immunobiology 2012, 217:468−475
67. Nielsen N, Pascal V, Fasth AE, Sundstrom Y, Galsgaard ED, Ahern D, Andersen M, Baslund B, Bartels EM, Bliddal H, Feldmann M, Malmstrom V, Berg L, Spee P, Soderstrom K: Balance between activating NKG2D, DNAM-1, NKp44 and NKp46 and inhibitory CD94/NKG2A receptors determine NK degranulation towards RA synovial fibroblasts. Immunology 2014, 142:581−593
68. Balsamo M, Scordamaglia F, Pietra G, Manzini C, Cantoni C, Boitano M, Queirolo P, Vermi W, Facchetti F, Moretta A, Moretta L, Mingari MC, Vitale M: Melanoma-associated fibroblasts modulate NK cell phenotype and antitumor cytotoxicity. Proc Natl Acad Sci U S A 2009, 106:20847−20852
69. Shi FD, Wang HB, Li H, Hong S, Taniguchi M, Link H, Van Kaer L, Ljunggren HG: Natural killer cells determine the outcome of B cell-mediated autoimmunity. Nat Immunol 2000, 1:245−251
70. Fujiu K, Nagai R: Contributions of cardiomyocyte-cardiac fibroblast-immune cell interactions in heart failure development. Basic Res Cardiol 2013, 108:357
71. Zhang J, Wu Y, Weng Z, Zhou T, Feng T, Lin Y: Glycyrrhizin protects brain against ischemia-reperfusion injury in mice through HMGB1-TLR4-IL-17A signaling pathway. Brain Res 2014, 1582:176−186
72. Wang JY, Shyur SD, Wang WH, Liou YH, Lin CG, Wu YJ, Wu LS: The polymorphisms of interleukin 17A (IL17A) gene and its association with pediatric asthma in Taiwanese population. Allergy 2009, 64:1056−1060
73. Jin R, Guo S, Wu L, Fan X, Ma H, Lowrie DB, Zhang J: Il17A autoantibody induced by recombinant protein Ag85A-Il17A. Appl Biochem Biotechnol 2013, 169:502−510
74. Wu X, Zeng Z, Xu L, Yu J, Cao Q, Chen M, Sung JJ, Hu P: Increased expression of IL17A in human gastric cancer and its potential roles in gastric carcinogenesis. Tumour Biol 2014, 35:5347−5356
75. Mantovani A: The chemokine system: redundancy for robust outputs. Immunol Today 1999, 20:254−257
76. Lukacs NW, Oliveira SH, Hogaboam CM: Chemokines and asthma: redundancy of function or a coordinated effort? J Clin Invest 1999, 104:995−999
77. Fujisawa T, Velichko S, Thai P, Hung LY, Huang F, Wu R: Regulation of airway MUC5AC expression by IL-1beta and IL-17A: the NF-kappaB paradigm. J Immunol 2009, 183:6236−6243
78. Chen XQ, Yu YC, Deng HH, Sun JZ, Dai Z, Wu YW, Yang M: Plasma IL-17A is increased in new-onset SLE patients and associated with disease activity. J Clin Immunol 2010, 30:221−225
79. Fujisawa T, Chang MM, Velichko S, Thai P, Hung LY, Huang F, Phuong N, Chen Y, Wu R: NF-kappaB mediates IL-1beta- and IL-17A-induced MUC5B expression in airway epithelial cells. Am J Respir Cell Mol Biol 2011, 45:246−252
80. Zhao N, Hao J, Ni Y, Luo W, Liang R, Cao G, Zhao Y, Wang P, Zhao L, Tian Z, Flavell R, Hong Z, Han J, Yao Z, Wu Z, Yin Z: Vgamma4 gammadelta T cell-derived IL-17A negatively regulates NKT cell function in Con A-induced fulminant hepatitis. J Immunol 2011, 187:5007−5014
81. Kong Q, Xue Y, Wu W, Yang F, Liu Y, Gao M, Lai W, Pan X: IL-22 exacerbates the severity of CVB3-induced acute viral myocarditis in IL-17A-deficient mice. Mol Med Rep 2013, 7:1329−1335
82. Ljunggren HG, Malmberg KJ: Prospects for the use of NK cells in immunotherapy of human cancer. Nat Rev Immunol 2007, 7: 329−339
83. Lee SK, Gasser S: The role of natural killer cells in cancer therapy. Front Biosci (Elite Ed) 2010, 2:380−391
84. Vivier E, Ugolini S, Blaise D, Chabannon C, Brossay L: Targeting natural killer cells natural killer T cells in cancer. Nat Rev Immunol 2012, 12:239−252